Optimum Photolysis in Taylor–Couette Flow

L. J. Forney
School of Chemical Engineering, Georgia Tech, Atlanta, GA 30332

J. A. Pierson
Georgia Tech Research Institute, Atlanta, GA 30332

Photolysis was studied in Taylor–Couette flow, and a similarity law proposed for the formation of a product from a fast photochemical reaction in the presence of laminar Taylor vortices. The concentration of the product formed depended on both the dosage of photons and a reaction-layer thickness, defined by the radiation penetration depth. In particular, for a given flow rate and radiation intensity, the UV photolysis of iodide produced a maximum concentration of the product triiodide, when the radiation penetration depth was equal to the velocity boundary-layer thickness. The latter conclusion provides optimum operating conditions to maximize yield in terms of the Taylor number or frequency of rotation.

Introduction

The absorption of electromagnetic radiation by a gas or liquid can increase the material temperature, cause fluorescence, as in the case of fluorescin, or produce a chemical change. In primary photochemical reactions the energy of the radiation measured in units of quanta is absorbed by the reacting species, that is, one quantum per molecule. The fate of the excited molecule leads to a number of possible secondary processes such as fragmentation or elevated electron states that can promote further chemical reactions (Considine, 1976).

The photochemical processing of liquids requires radiation absorption through transparent reactor walls. The efficiency of such processes is improved with enhanced liquid-surface renewal and contacting with the reactor walls, in particular, for liquid reagents that strongly absorb the applied radiation. For example, conventional plug-flow reactors operating in laminar flow provide poor results if the absorptivity of the applied radiation is large since liquid dosage is negligible in the fluid interior. Attempts to redirect the flow with vanes or static mixing elements that introduce turbulence at a low Reynolds number cause potential scale-up problems in addition to obscuring the radiation flux. Moreover, alternative geometries, such as a stirred tank, will reduce a process photoefficiency because of both a significant increase in the radiation path length and a reduction in the surface-to-volume ratio, unless a large number of radiation sources are placed within the reactor interior.

Correspondence concerning this article should be addressed to L. J. Forney.

An elegant alternative to the conventional reactors just described is the case of flow between two concentric cylinders, of which the inner cylinder is rotating and the outer cylinder is at rest. In such a flow the unstable stratification caused by centrifugal forces forms counterrotating vortices, known as Taylor vortices (Taylor, 1923), whose axes are circumferential, as shown in Figure 1. In fact, Kataoka et al. (1975) demonstrated that such Taylor–Couette flows produce nearly ideal plug-flow characteristics. The potential of Taylor–Couette geometries for chemical processing by enhanced heat and mass transfer was also demonstrated by Cohen and Marom (1983).

Existing published experimental results for the surface mass-transfer characteristics of homogenous fluids in Taylor–Couette flows are summarized by Baier et al. (1999). The latter study uses CFD results and the boundary-layer theory to predict experimental mass-transfer coefficients or Sherwood numbers of the form discussed by Holeschovsky and Cooney (1991). Much less work has been done to characterize mass transfer in nonhomogeneous fluids, that is, between immisible liquids such as dispersed and continuous phases considered in a recent study by Forney et al. (1999, 2002a) or the novel two-fluid (without dispersion) Taylor vortex extractor described by Baier et al. (2000).

Three previous experiments are recorded to characterize photoefficiencies in Taylor–Couette flow. Algal photosynthesis was investigated by Miller et al. (1964), who concluded that higher photoefficiencies were obtained with larger cell suspension densities. Recently, Sczechowski et al. (1995)

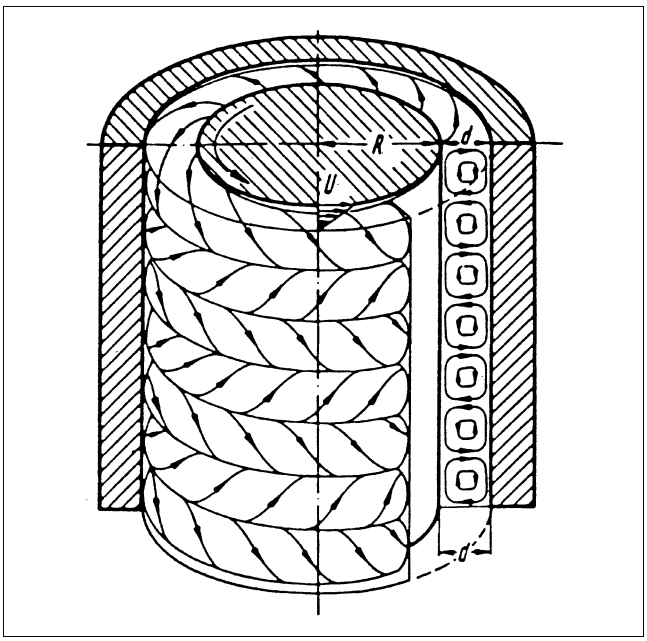

Figure 1. Taylor vortices between two concentric cylinders.

Inner cylinder rotating, outer cylinder at rest; d—width of annular gap (Schlichting, 1979).

studied heterogeneous photocatalysis to improve aqueous oxidation processes. As in the earlier experiment, the latter study concluded that improved photoefficiencies were obtained with larger weight loadings of the titanium dioxide photocatalyst. Finally, the author's motivation for the present study was the observation that the dimerization of nucleic acid strands in pathogens leading to their inactivation was most efficient at low rpm, that is, Taylor–Couette flow as described by Forney et al. (2002b).

In this article the geometry of a laminar Taylor–Couette reactor is explored in the context of photochemical reactions. In particular, fluid is irradiated through the transparent cylindrical stator of a Taylor–Couette device. The yield of fast UV-induced triiodide formed from aqueous solutions of potassium iodide was measured for various operating conditions. These results clearly indicate a number of advantages for the Taylor column. Moreover, the criterion for optimum operating conditions is proposed and supported by both present and previous results.

Photochemistry

The reaction used in the present study is the fast UV photolysis of aqueous iodide, producing triiodide. Concentrated KI solutions are optically opaque at wavelengths of 254 nm and act as photon counters (Rahn et al., 1999). UV absorption by iodide leads to an aqueous or solvated electron via a charge transfer-to-solvent reaction and the formation of an excited iodine atom. The essential reactions are listed below

$$I^- + h\nu \rightarrow I^* + e^- \quad (1)$$

$$I^* + e^- \rightarrow I^- \quad (2)$$

$$2I^* + I^- \rightarrow I_3^- \quad (3)$$

As noted, the UV-induced formation of triiodide is potentially limited by the back reaction of Eq. 2. The quantum yield for triiodide is significantly increased, however, by the addition of potassium iodate. In the presence of iodate, scavenging of the bulk electron occurs and the following additional reaction is proposed (Rahn, 1997)

$$IO_3^- + e^- + 2H_2O \rightarrow IO^- + H_2O_2 + OH^* + OH^- \quad (4)$$

The yield of the triiodide photoproduct is easily monitored by spectrophotometry at either 350 or 450 nm, depending on the concentration. The quantum yield of $\varphi = 0.75$ mol I_3/einstein is relatively constant with either temperature or reagent iodide concentrations (Rahn et al., 1999). With the addition of a borate buffer (pH 9.25) to minimize thermal oxidation, stock solutions of 0.6 M KI and 0.1 M KIO_3 with the borate buffer are stable and insensitive to ambient light in the visible spectrum.

Taylor Couette Flow

Chilton–Colburn analogy

Radial mass transfer in Taylor–Couette flow has been documented in terms of a Sherwood number (Sh) of the form

$$Sh \; \alpha \; Ta^{1/2} Sc^{1/3} \quad (5)$$

where the Taylor number

$$Ta = (\omega R d/\nu)(d/R)^{1/2} \quad (6)$$

The indicated exponents in Eq. 5 were determined by a number of experiments (Mizushina, 1971; Kataoka et al., 1977; Coeuret and Legrand, 1981; Holeschovsky and Cooney, 1991) and also confirmed by the recent numerical predictions of Baier et al. (1999). We also note that the torque coefficient, C_M, for Taylor–Couette flow is of the form

$$C_M = 2M/(\pi\rho\omega^2 R^4 h) \; \alpha \; Ta^{-1/2} \quad (7)$$

as shown in Figure 2 for the range of Taylor numbers $Ta_c < Ta < 400$, where the critical Taylor number, $Ta_c = 41$, indi-

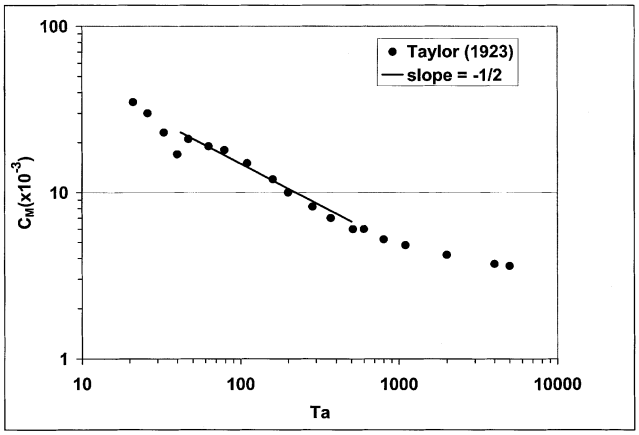

Figure 2. Torque coefficient vs. Taylor number.

cates the onset of laminar vortices (Schlichting, 1979). Here, the moment $M = \tau(2\pi R^2 h)$, and τ is the shear stress on the rotor.

Equations 5 and 7 suggest that the transport coefficients in laminar Taylor–Couette flows are correlated by a Chilton–Colburn analogy of the form

$$J_D = Sh/(TaSc^{1/3}) = C_M/2 \tag{8}$$

for the values $40 < Ta < 400$ and the Schmidt number $Sc = \nu/\bar{D} > 1$. These conclusions are consistent with laminar heat-transfer correlations on a spinning disk, but with Ta replaced by the Reynolds number based on the disk angular velocity and diameter (Schlichting, 1979; Bird et al., 2002).

Now consider a laminar boundary layer with a linear velocity and concentration profile (film model) on the surface of a Taylor–Couette flow ($Ta > Ta_c$). Since the mass-transfer coefficient $k_c \alpha \bar{D}/\delta_c$ and the Sherwood number

$$Sh \alpha k_c d/\bar{D} \tag{9}$$

where δ_c is the concentration boundary-layer thickness, d is the gapwidth, and $\bar{D}$ is the solute molecular diffusivity, one obtains

$$Sh \alpha d/\delta_c \alpha (d/\delta)(\delta/\delta_c) \tag{10}$$

Since a boundary-layer analysis confirmed by experiment suggests $\delta_c/\delta \alpha Sh^{1/3}$, one obtains a ratio of characteristic reactor length d-to-velocity boundary thickness

$$d/\delta \alpha Ta^{1/2} \tag{11}$$

for $Ta > Ta_c$.

Attempts to obtain Eq. 11 by stretching the characteristic lengths d or δ for a boundary layer on a flat plate by a factor of $(d/R)^{1/2}$ were unsuccessful by the present authors. There is some evidence, however, that the Sherwood number $Sh \alpha Ta^{1/2}Sc^{1/3}(d/R)^{0.17}$ from the mass-transfer experiments of Holeschovsky and Cooney (1991) but, again, the exponent magnitude of 0.17 is inconsistent with our attempted boundary analysis that would suggest larger values.

Dimensional arguments

Fast photochemical reactions must occur near transparent reactor walls. The thickness of the reaction layer, however, is not confined to a fraction of the velocity boundary thickness, but rather to the radiation penetration depth. The latter depth, in fact, can exceed both the boundary thickness or characteristic reaction dimension, depending on the absorbance of the reacting solution.

Since the solution absorbance is defined by

$$A = \lambda \epsilon C \tag{12}$$

where the intensity of radiation is $I/I_o = 10^{-A}$, ϵ is the extinction coefficient, C is the absorbing species, and λ is the radiation depth, the reaction layer is, therefore, confined to a layer on the order of

$$\lambda \alpha 1/\epsilon C \tag{13}$$

as shown in Figure 3.

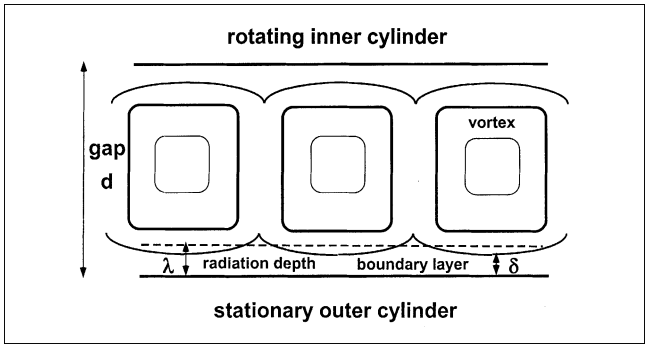

Figure 3. Velocity boundary-layer thickness (magnified) and radiation penetration depth within annular gap.

An additional dimensional parameter is the maximum possible concentration of a photochemical product formed. The latter is equal to the product of the number of photons introduced into the reactor and the quantum efficiency of the reaction. The maximum concentration of the product formed is thus

$$Cm = nI_o A_l \varphi/\gamma q \tag{14}$$

where n is the number of lamps, I_o is the intensity of radiation (W/cm^2), A_l is the area of a single lamp, φ is the reaction quantum efficiency (mol product/einstein), q is the reactor volume flow rate, and γ (J/einstein) is the conversion factor from a mol of photons to joules of energy.

Dimensional arguments suggest that the concentration of photochemical product formed C_ω is of the form

$$C_\omega/C_i(I) \alpha f\left[Cm/C_i(I), \lambda/\delta\right] \tag{15}$$

provided the Taylor number $Ta > 0$, where $C_i(I)$ is the concentration of reactant iodide in the inlet stream. Simplifying Eq. 15 somewhat, since a mass balance implies $C_\omega \alpha Cm$, one obtains

$$C_\omega/C_i(I) \alpha Cm/C_i(I)[f(\lambda/\delta)] \tag{16}$$

Defining Co as the product concentration with no rotation, one now obtains an expression that isolates the effects of rotation in the form of the dimensionless quantity

$$(C_\omega - Co)/Co = f(\lambda/\delta) \tag{17}$$

Experimental Apparatus

A Taylor vortex column, as shown in Figure 4 was constructed, consisting of a bronze rotor 3.43 cm in diameter by 5 cm in length centered within a fused quartz beaker with an

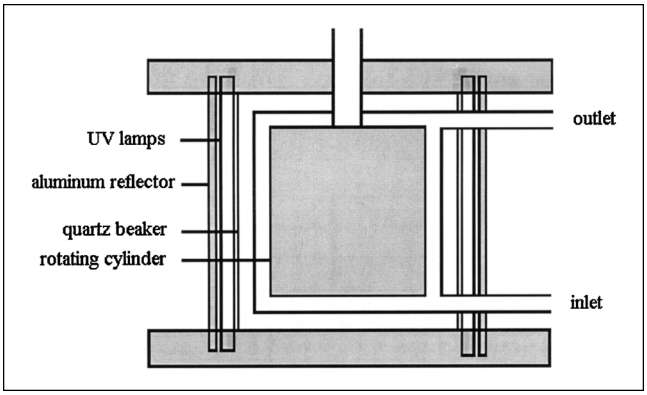

Figure 4. Experimental apparatus.

inside diameter of 4.1 cm, providing a gapwidth of $d = 0.334$ cm. The holdup volume (irradiated) was 12 mL, with a range of flow rates between $15 < q < 50$ mL/min. Four cold-cathode, low-pressure mercury UVC lamps (Gilway Technical Lamp) with effective lengths of 3.1 cm were positioned around the quartz beaker and surrounded by an aluminum reflector with an UV radiation reflectivity of over 90% as shown in Figure 4. The intensity of radiation for each lamp (wavelength ~ 254 nm) was rated at 4.0 mW/cm^2 at one cm from the lamp surface, providing a range of power input from 0.78 W to 0.31 W, depending on the number of lamps engaged.

A solution of 0.6 M potassium iodide (KI) and 0.1 M potassium iodate (KIO_3) buffered (pH 9.25) with borate was pumped through the Taylor column. The absorbance of triiodide at the outlet was measured at either 350 or 450 nm for low or high concentrations, respectively, depending on the number of lamps engaged or liquid flow rate. The rpm of the rotor, controlled by a permanent magnet DC motor, was varied between $0 < \text{rpm} < 75$, providing a Taylor number covering the range $0 < Ta < 200$, as shown in Figure 5.

The triiodide absorbance in Figure 5, as expected, clearly indicates a large increase of roughly 60% for Taylor numbers $Ta > Ta_c$, where the lower limit of $Ta_c \sim 40$ corresponds to the onset of Taylor vortices at low axial Reynolds numbers. Since the cross-sectional area for the flow within the gap is 3.9 cm^2, the axial Reynolds number was $Re < 10$ for all experiments, and, thus, had no effect on the critical Ta_c.

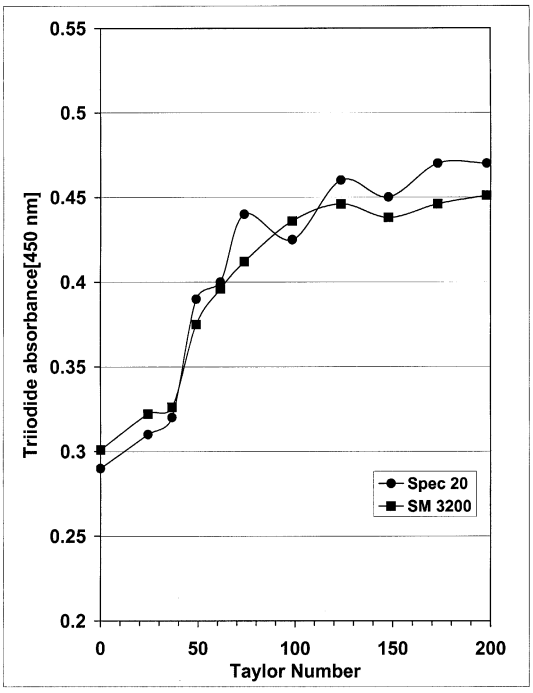

Figure 5. Measurements of triiodide absorbance vs. Taylor number with two spectrophotometers.

Flow rate is 31.2 mL/min with inlet aqueous concentrations of 0.6 M KI and 0.1 M KIO_3.

Results and Discussion

Plug-flow reactor

When the Taylor number $Ta > Ta_c$ and laminar vortices are present within the Taylor column, the flow can best be described as approximating that of an ideal plug-flow reactor (Kataoka et al., 1975). Assuming a zero-order rate expression at steady state, one obtains

$$udC/dx = r \tag{18}$$

where the constant rate [mol/L-s]

$$r = nI_o A_l \varphi/\gamma V \tag{19}$$

and V is the irradiated holdup volume of the reactor. Thus, the concentration of triiodide formed from Eq. 18 with $dx/u = dV/q$ is

$$C(I_3) = \beta rV/q \tag{20}$$

where the factor $\beta < 1$ accounts for both the loss of input radiant energy to liquid heating and surface absorption and the effects of back reactions from tri-iodide to iodide depleting the product, as described later.

Figure 6 illustrates the validity of Eq. 16 for the outlet triiodide concentration for increasing flow rates at fixed rpm

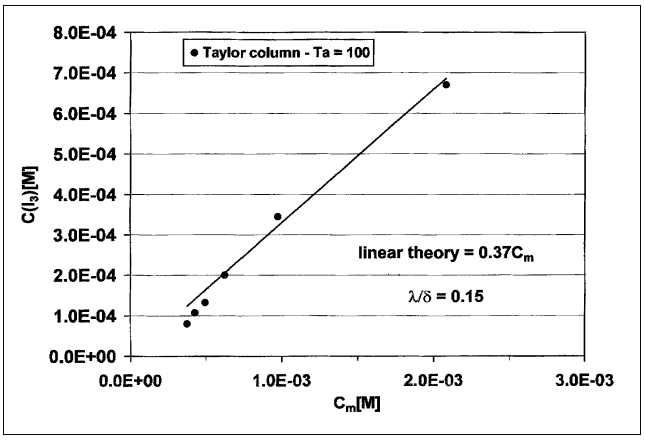

Figure 6. Normalized outlet triiodide concentration vs. nondimensional dosage.

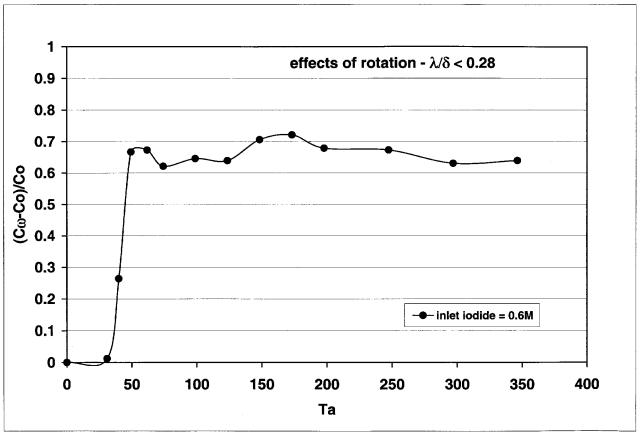

Figure 7. Fractional increase in outlet triiodide concentration vs. Taylor number.

Radiation dosage is 0.164 W and flow rate is 16 mL/min.

($Ta = 100$) and the standard stock solution ($C_i(I) = 0.6$ M iodide), where Cm is defined by Eq. 14. It is evident from Figure 6 that although the photoefficiency of the reactor is high, $C_i(I) \gg Cm$, so that axial variations in the iodide reactant $C_i(I)$, and, thus, the radiation penetration depth, are small, which is consistent with the analysis.

Effects of rotation

In the present work, the effects of rotation are isolated by comparing the product concentration at fixed Taylor numbers $Ta > Ta_c$, with the product formed at zero rpm or $Ta = 0$. Because of the large surface-to-volume ratio for the reactor, one would expect a considerable enhancement in the magnitude of the transport coefficients without vortices. One such plot of experimental data is shown in Figure 7, where it is demonstrated that a nearly constant 70% improvement in product yield occurs for all $Ta > Ta_c$.

Figure 8 compares the percentage increase in the reaction product at fixed $Ta = 100$ for various values of the radiation dosage. These data were obtained by engaging one to five

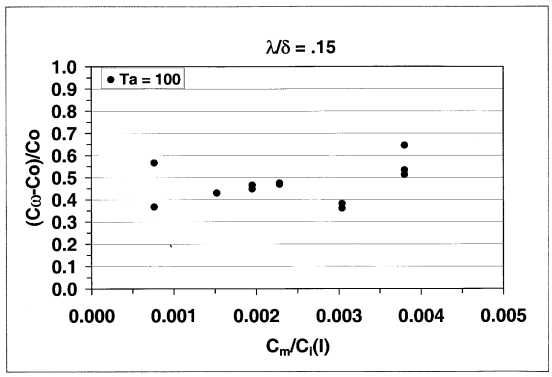

Figure 8. Fractional change in outlet triiodide concentration for a radiation dosage from 0.078 W to 0.31 W.

Inlet concentration is 0.6 M KI and 0.1 M KIO_3. Lamp sequence was varied.

UV lamps and changing the flow rate between 16 and 32 mL/min. There is some scatter in the data, possibly due to channeling through the reactor for the $Ta = 0$ case, since the reactor inlet and outlet were located on the same side but 45° apart. Thus, the sequence of lamps in the circumferential direction was varied for several experiments with the same total power input leading to the indicated scatter. However, it is apparent from Figure 8 that the concentration of the product formed due to rotation is independent of the dosage of radiation supplied, as suggested by Eq. 17.

Optimum rotation

The similarity law proposed by Eq. 17 was tested by varying the reactant concentration, that is, the concentration of iodide fed to the reactor inlet. Since the absorbance $A = \lambda \epsilon C_i(I)$ is 200 for a 0.6 M KI and 0.1 M KIO_3 solution, the extinction coefficient ϵ at a wavelength of 254 nm was calculated to be $\epsilon = 333\ \mathrm{M^{-1}cm^{-1}}$ (Rahn et al., 1999). Setting the absorbance $A = 1$, which represents a radiation depth over which 90% of the UV photons are absorbed, one calculates the radiation depth to be $\lambda = 1/\epsilon C_i(I)$.

The stock solution of 0.6 M KI and 0.1 M KIO_3, along with a series of additional solutions with KI and KIO_3 in the same ratio but diluted by a factor of up to 100, were fed to the reactor. The product triiodide concentration was measured at both $Ta = 0$ and 100 for each inlet solution, and these results are plotted in Figure 9. The normalized fractional change in the product I_3^- concentration is plotted in Figure 10 as a function of the ratio of radiation depth-to-velocity boundary thickness.

As clearly demonstrated in Figure 10, the reaction yield is inhibited if the reaction layer lies within the velocity boundary layer or $\lambda/\delta \ll 1$. Under these circumstances the large concentration of I_3^- within the boundary is reduced by the solvated electron e_{aq}^- back to I^- via the reaction (Dainton and Logan, 1965)

$$e_{aq}^- + \mathrm{I}_3^- \rightarrow \mathrm{I}_2^- + \mathrm{I}^- \tag{21}$$

and the product yield of I_3^- is diffusion limited.

In contrast, if the reaction-layer thickness is greater than the velocity boundary layer or $\lambda/\delta \gg 1$, the product I_3^- is formed throughout the gap and the advantages of the circulating vortices are substantially reduced. It should be noted that the left data point in Figure 10 corresponds to a reaction layer that is 15% of the velocity boundary thickness, where the latter is 10% of the gapwidth. In contrast, the right data point in Figure 10 represents a radiation depth that is 150% of the gapwidth d.

At the optimum operating conditions $\lambda/\delta = 1$ one obtains a maximum 150% increase in the product concentration. Under the latter constraint, if

$$\lambda/\delta = Ta^{1/2}/\left[d\epsilon C_i(I)\right] \tag{22}$$

setting $\lambda/\delta = 1$, one obtains an optimum frequency $f_{op}(\mathrm{Hz^{-1}})$ of rotation equal to

$$f_{op} = (\nu/2\pi)(d/R)^{1/2}\epsilon^2 C_i^2(I) \tag{23}$$

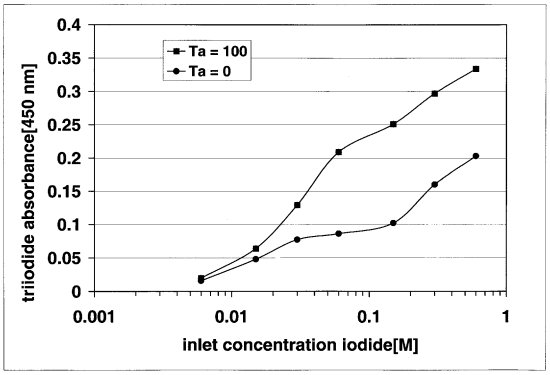

Figure 9. Absorbance of outlet triiodide concentration at both *Ta* = 0 and 100 vs. inlet iodide concentration; flow rate is 16 mL/min.

Previous experiments

Sczechowski et al. (1995) studied a heterogeneous photocatalysis process within a Taylor column. In these experiments, a semiconductor photocatalyst powder, titanium dioxide, was illuminated with long-wave UV light to produce a strong oxidizing species such as hydroxyl radicals. The decomposition of total organic carbon (TOC) by such species was measured as a function of operating conditions for a Taylor column, mainly T_iO_2 powder loading and rotation rate.

The experimental determination of 90% attenuation in 2 mm of a 1-g/L slurry of T_iO_2 provided a radiation penetration depth $\lambda \alpha 1/C(T_iO_2)$ for a series of four T_iO_2 loadings from 0.5 g/L to 10 g/L. Each T_iO_2 loading was subjected to a *Ta* range from $124 < Ta < 7{,}445$. The raw data in terms of the rate of TOC removal for a fixed set of operating conditions was determined by sampling at four ports along the axis of the reactor designed with a gapwidth $d = 1$ cm.

Calculating δ, the velocity boundary-layer thickness, from Eq. 11 by introducing their recorded rotator rpm and combining these results with the calculated radiation penetration depth, one obtains the plot of Figure 11. Estimates of the values of λ/δ for maximum TOC removal are plotted in Fig-

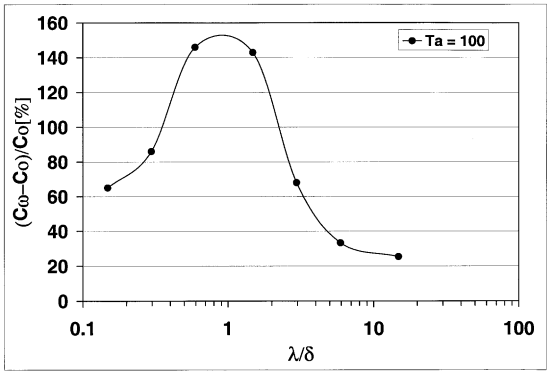

Figure 10. Percent change in outlet triiodide concentration vs. ratio of radiation penetration depth-to-velocity boundary-layer thickness.

(Data taken from Figure 9).

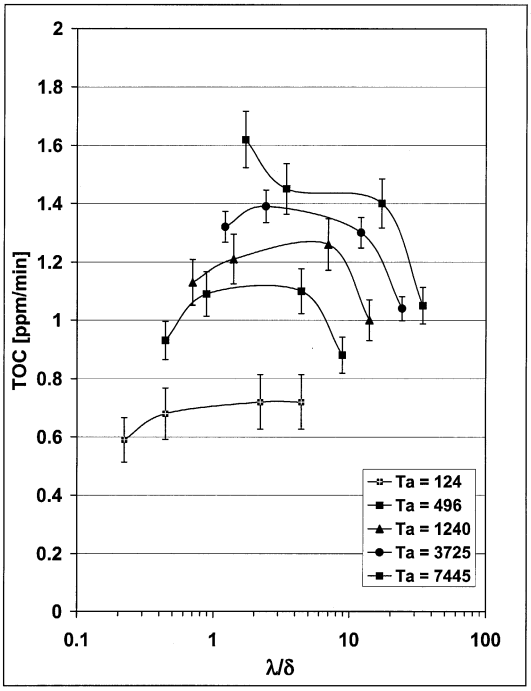

Figure 11. Removal rate of total organic carbon vs. ratio of radiation depth-to-velocity boundary-layer thickness.

[Data replotted from Sczechowski et al. (1995)].

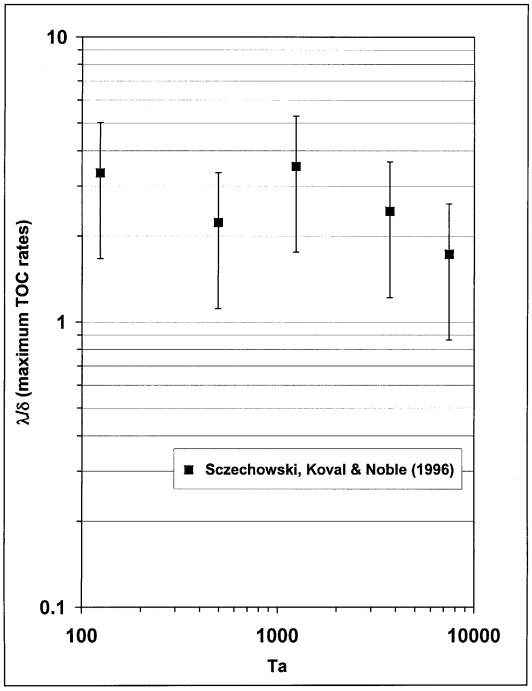

Figure 12. Ratio of radiation penetration depth-to-velocity boundary-layer thickness at maximum TOC removal vs. Taylor number.

(Data taken from Figure 11).

ure 12. Clearly, there is much scatter to these plots, but the data confirm the suggested similarity law of Eq. 17.

Conclusions

Taylor–Couette flow provides excellent liquid-surface renewal for the application of electromagnetic waves to chemical processing. The photoefficiency of such processes is affected by the depth of radiation penetration into the fluid relative to the velocity boundary-layer thickness. The secondary flow caused by the presence of laminar vortices decreases the boundary-layer thickness so that the dosage of radiation is substantially increased for fluids with large radiation absorptivities. The maximum photoefficiencies occur when the radiation penetration depth is equal to the boundary-layer thickness.

Acknowledgment

The authors acknowledge the support of FoodPAC from Georgia's Traditional Industries Program for Food Processing under contract GTRI # N-5430-200.

Notation

A = absorbance
A_l = single UV lamp area, cm^2
C = triiodide concentration, mol/L
C_i = inlet iodide concentration, mol/L
C_m = maximum triiodide from all photons, mol/L
C_M = torque coefficient
Co = outlet triiodide concentration $Ta = 0$, mol/L
C_ω = outlet triiodide concentration $Ta > 0$, mol/L
d = gap width, cm
D = molecular diffusivity, cm^2/s
f_{op} = optimum rotation rate, Hz^{-1}
h = rotor length, cm
I = radiation intensity, W/cm^2
I_o = initial radiation intensity, W/cm^2
J_D = j-factor, mass transfer
k_c = mass-transfer coefficient, cm/s
n = number of lamps
q = volume flow rate, mL/min
r = rate constant, mol/L·s
R = radius of rotating cylinder, cm
Re = axial Reynolds number in gap
Sc = Schmidt number
Sh = Sherwood number
Ta = Taylor number
Ta_c = critical Taylor number for laminar vortices
TOC = total organic carbon, ppm
u = mean axial fluid velocity, cm/s
V = irradiated reactor holdup volume, mL
x = axial position in reactor, cm

Greek letters

γ = conversion factor, 4.72×10^5 J/einstein
β = nondimensional factor
ϵ = extinction coefficient, $M^{-1} \cdot cm^{-1}$
δ = velocity boundary thickness, cm
δ_c = concentration boundary-layer thickness, cm
λ = radiation penetration depth, cm
ω = angular velocity of cylinder, rad/s
φ = quantum efficiency, 0.75 mol triiodide/einstein

Literature Cited

Baier, G., T. M. Grateful, M. D. Graham, and E. N. Lightfoot, "Prediction of Mass Transfer in Spatially Periodic Systems," *Chem. Eng. Sci.*, **54**, 343 (1999).

Baier, G., T. M., M. D. Graham, and E. N. Lightfoot, "Mass Transport in a Novel Two-Fluid Taylor Vortex Extractor," *AIChE J.*, **46**, 2394 (2000).

Bird, R. B., W. E. Stewart, and E. N. Lightfoot, *Transport Phenomena*, 2nd ed., Wiley, New York (2002).

Coeuret, F., and J. Legrand, "Mass Transfer at the Electrodes of Concentric Cylindrical Reactors Combining Axial Flow and Rotation of the Inner Cylinder," *Electrochim. Acta*, **26**, 865 (1981).

Cohen, S., and D. M. Marom, "Experimental and Theoretical Study of a Rotating Annular Flow Reactor," *Chem. Eng. J.*, **27**, 87 (1983).

Considine, D. M., ed., *Van Nostrand's Scientific Dictionary*, 5th ed., Van Nostrand Reinhold, New York, p. 1764 (1976).

Dainton, F. S., and S. R. Logan, "Primary Process in the Photolysis of the Iodide Ion in Aqueous Solution," *Proc. Roy. Soc. London*, **287**, 281 (1965).

Holeschovsky, U. B., and C. L. Cooney, "Quantitative Description of Utrafiltration in a Rotational Filtration Device," *AIChE J.*, **37**, 1219 (1991).

Forney, L. J., A. H. P. Skelland, J. F. Morris, and R. Hall, "Taylor Vortex Column: Large Shear for Two Phase Flows," AIChE Meeting, Dallas, TX (1999).

Forney, L. J., A. H. P. Skelland, J. F. Morris, and R. Hall, "Taylor Vortex Column: Large Shear for Liquid-Liquid Extraction," *Sep. Sci. Technol.*, **37**, 2967 (2002a).

Forney, L. J., J. A. Pierson, and C. Goodridge, "Development of an Advanced UV Disinfection Technology," Annu. Rep. for FoodPAC, Georgia Tech Research Institute, Atlanta, GA (2002b).

Gilway Technical Lamp, Catalog No. 169 (2001).

Kataoka, K., H. Doi, T. Hongo, and M. Futagawa, "Ideal Plug-Flow Properties of Taylor Vortex Flow," *J. Chem. Eng. Jpn.*, **8**, 472 (1975).

Kataoka, K., H. Doi, and T. Komai, "Heat/Mass Transfer in Taylor Vortex Flow with Constant Axial Flow Rates," *Int. J. Heat Mass Trans.*, **20**, 57 (1977).

Miller, R. L., A. G. Fredrickson, A. H. Brown, and H. M. Tsuchiya, "Hydromechanical Method to Increase Efficiency of Algal Photosynthesis," *Ind. Eng. Chem. Process Des. Dev.*, **3**, 134 (1964).

Mizushina, T., "The Electrochemical Method in Transport Phenomena," *Adv. Heat Trans.*, **7**, 86 (1971).

Rahn, R. O., "Potassium Iodide as a Chemical Actinometer for 254 nm Radiation: Use of Iodate as an Electron Scavenger," *Photochem. Photobiol.*, **66**, 450 (1997).

Rahn, R. O., P. Xu, and S. L. Miller, "Dosimetry of Room-Air Germicidal (254nm) Radiation Using Spherical Actinometry," *Photochem. Photobiol.*, **70**, 314 (1999).

Schlichting, H., *Boundary Layer Theory*, 7th ed., McGraw-Hill, New York (1979).

Sczechowskii, J. G., C. A. Koval and R. D. Noble, "A Taylor Vortex Reactor for Heterogeneous Photocatalysis," *Chem. Eng. Sci.*, **50**, 3163 (1995).

Taylor, G. I., "Stability of a Viscous Liquid Contained Between Two Rotating Cylinders," *Philos. Trans. Roy. Soc. London A*, **223**, 289 (1923).

Manuscript received May 20, 2002, and revision received Sept. 30, 2002.